Laser Sputtering Generation of B_2 for ESR Matrix Isolation Studies: Comparison with ab Initio CI Theoretical Calculations

Lon B. Knight, Jr.,*† B. W. Gregory,† S. T. Cobranchi,† David Feller,‡ and E. R. Davidson‡

Contribution from the Chemistry Departments, Furman University, Greenville, South Carolina 29613, and Indiana University, Bloomington, Indiana 47405.
Received December 1, 1986

Abstract: The $^{11}B_2$ molecule has been trapped in neon and argon matrices at 5 ± 1 K for ESR (electron spin resonance) investigations. Laser sputtering from solid boron was used to generate the B_2 molecule whose ground electronic state has been established experimentally for the first time to be $^3\Sigma_g^-$. The ESR nuclear hyperfine parameters for B_2 and B atoms have been compared with the results of ab initio CI theoretical calculations. Good agreement between theory and experiment is found for the dipolar component of the **A** tensor but not for the small and difficult to calculate isotropic hfs. Reasons that make the Fermi contact term especially difficult to calculate in this particular case are presented. The argon matrix ESR results yield the following magnetic parameters for $^{11}B_2$ in its ground electronic state: $g_\parallel = g_\perp = 2.0015$ (4); $A_\parallel = \pm 11$ (1) MHz and $A_\perp = \pm 27.4$ (3) MHz for ^{11}B and the zero field parameter; and the D value is 3633 (3) MHz. As discussed, the most reasonable signs for the A values are $A_\parallel < 0$ and $A_\perp > 0$. The neon matrix value of D was found to be 3840 (3) MHz and $A_\perp$ in neon is ±26.6 (3) MHz.

The ground electronic state for the diatomic boron molecule, B_2, has not been completely established by experiment. Electronic emission bands were assigned to a $\Sigma \rightarrow \Sigma$ type transition in early spectroscopic studies by Douglas and Herzberg (DH) which produced B_2 in a helium discharge containing boron trichloride.[1] The observation of this DH band by optical absorption in an argon matrix at 10 K by Graham and Weltner confirmed the Σ ground-state assignment.[2] Attempts by these investigators to observe the argon matrix ESR (electron spin resonance) spectrum of B_2 were not successful, hence the multiplicity of the ground Σ state could not be determined. The B_2 molecule in this earlier matrix study was produced by conventional high temperature vaporization methods, and presumably its concentration was too low for the observation of a powder sample for such a highly anisotropic radical. The lack of ESR signals at X-band microwave frequencies was attributed to a zero-field splitting (zfs) greater than 4 cm^{-1}.[2]

An earlier calculation indicated that the ground state of B_2 was $^5\Sigma_u^-$ which occurred about 12000 cm^{-1} below the $^3\Sigma_g^-$ state.[3] A later CI calculation found the quintet to lie only 1100 cm^{-1} below the triplet state.[4] More recent calculations conclude that the $^3\Sigma_g^-$ state, lying 1300 cm^{-1} below the $^5\Sigma_u^-$ state, is the ground electronic state.[5] The neon and argon matrix ESR results presented in this report confirm the $^3\Sigma_g^-$ as the ground state. A detailed SCF and CI calculation of the isotropic and dipolar nuclear hyperfine interaction (hfi) has been conducted for this $^3\Sigma_g^-$ state and compared to the ESR results. The calculated dipolar interaction shows excellent agreement with experiment while the small isotropic interaction resulting from the near cancellation of inner and valence shell contributions is noticeably different from the matrix observation. This nuclear hfi comparison between experiment and theory at the ab initio CI level is apparently the first one reported for a high-spin radical.

The generation of boron vapor at high concentrations by conventional high temperature methods is notoriously difficult given the refractory nature of boron, its high reactivity, and containment problems associated with molten boron above 2000 K. The ESR matrix experiments described in this report utilized pulsed laser sputtering of boron for the generation of B_2 which probably forms during the matrix deposition process from boron atoms. High temperature mass spectrometric measurements indicate that the relative concentration of $B_{2(g)}$ in the atomic vapor is approximately 10^{-4}.[6] The use of reactive laser sputtering (sputtering of metals under reactive gas flow conditions) in combination with the rare gas matrix ESR method has been used in our laboratory for several recent studies of highly reactive ion and neutral radicals, including AlH^+ and AlD^+,[7] AlF^+,[8] BF^+,[9] CH_3AlF, HAlOH, HCuF, and CH_3CuF.[10] The matrix ESR method, radical generation techniques, and related theoretical topics have been presented in other reports.[11-15]

Experimental Section

The ESR matrix apparatus used in our laboratory for trapping neutral and ion radicals in solid rare gases near 4 K has been described previously.[16] Figure 1 shows the relative locations of the copper matrix deposition surface, ESR cavity, and the boron target. Frequency doubled output from a Nd:YAG laser (Spectra Physics DCR-2A) at 532 nm was focused to approximately 1 mm on the boron target which is located 2 cm from the 5 K matrix deposition surface. Typical sputtering conditions were 40 mJ per pulse at a 10 Hz repetition rate. During the course of a 30-min deposition, the laser was moved slowly over the boron target by changing the position of the focusing lens mounted on an X-Y translator. A continuous flow of matrix gas (neon or argon) at 5.0 sccm was maintained during the pulsed sputtering process.

The boron target, mounted on an O-ring sealed shaft, was moved away from the matrix target area following deposition. This allows the helium Dewar to be lowered about 7 cm by means of a hydraulic system so that the attached matrix sample can be positioned in the X-band microwave cavity which is located inside the high-vacuum chamber. A 9-in. electromagnet (3.5 in. air gap) mounted on tracks is rolled into position for

(1) Douglas, A. E.; Herzberg, G. *Can. J. Res.* **1940**, *A18*, 165.
(2) Graham, W. R. M.; Weltner, W., Jr. *J. Chem. Phys.* **1976**, *65*, 1516.
(3) Padgett, A. A.; Griffing, V. *J. Chem. Phys.* **1959**, *30*, 1286.
(4) Bender, C. F.; Davidson, E. R. *J. Chem. Phys.* **1967**, *46*, 3313.
(5) Dupuis, M.; Liu, B. *J. Chem. Phys.* **1978**, *68*, 2902.
(6) Verhaegen, G.; Drowart, J. *J. Chem. Phys.* **1962**, *37*, 1367.
(7) Knight, L. B., Jr.; Cobranchi, S. T.; Gregory, B. W.; Earl, E. *J. Chem. Phys.*, in press.
(8) Knight, L. B., Jr.; Earl, E.; Ligon, A. R.; Cobranchi, D. P.; Woodward, J. R.; Bostick, J. M.; Davidson, E. R.; Feller, D. *J. Am. Chem. Soc.* **1986**, *108*, 5065.
(9) Knight, L. B., Jr.; Ligon, A.; Cobranchi, S. T.; Cobranchi, D. P.; Earl, E.; Feller, D.; Davidson, E. R. *J. Chem. Phys.* **1986**, *85*, 5437.
(10) Knight, L. B., Jr.; Cobranchi, S. T.; Gregory, B. W.; Earl, E. to be published.
(11) Weltner, W., Jr. *Magnetic Atoms and Molecules*; Van Nostrand-Reinhold Co.: New York, 1983.
(12) Knight, L. B., Jr. *Acc. Chem. Res.*, in press.
(13) Gordy, W. *Theory and Applications of Electron Spin Resonance*; Wiley and Sons: New York, 1980.
(14) Knight, L. B., Jr.; Ligon, A.; Woodward, J. R.; Feller, D.; Davidson, E. R. *J. Am. Chem. Soc.* **1985**, *107*, 2857.
(15) Kasai, P. H. *Acc. Chem. Res.* **1971**, *4*, 329.
(16) Knight, L. B., Jr.; Steadman, J. *J. Chem. Phys.* **1982**, *77*, 1750.

0002-7863/87/1509-3521$01.50/0

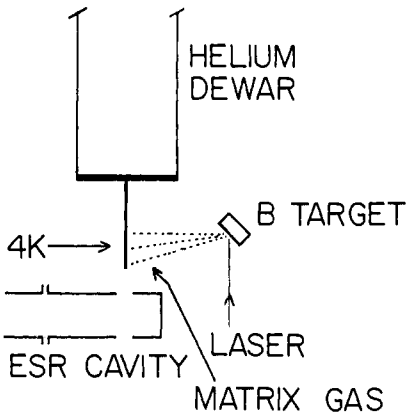

Figure 1. ESR apparatus for trapping laser sputtered products in rare gas matrices at 5 ± 1 K. The boron (B) target is located about 2 cm from the copper deposition surface which is lowered into the X-band microwave cavity for recording ESR spectra. The apparatus is contained within the gap of a 9-in. electromagnet and the 100 kHz modulation coils are attached to the cavity inside the vacuum system.

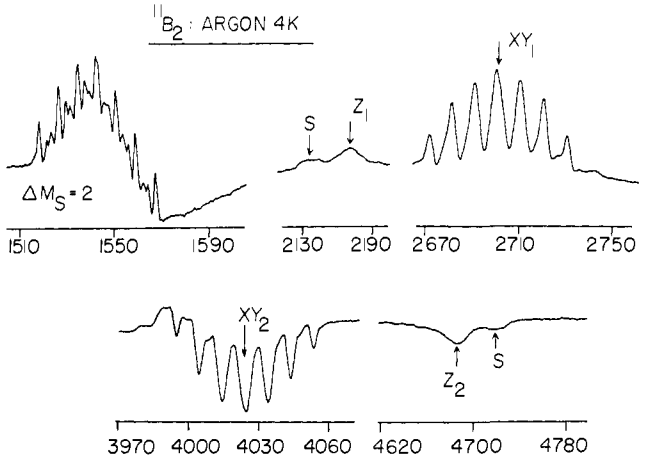

Figure 2. The overall ESR spectrum is shown for the $^{11}B_2$ radical in its $^3\Sigma_g^-$ ground electronic state trapped in an argon matrix at 5 ± 1 K. The XY_1 and XY_2 features are the perpendicular ($\theta = 90°$) transitions for $\Delta M_s = \pm 1$; Z_1 and Z_2 are the parallel ($\theta = 0°$) transitions. The weaker features labeled "S" result from an alternate trapping site in the argon lattice. See text. The $\Delta M_s = 2$ and the perpendicular transitions show septet nuclear hyperfine patterns resulting from two equivalent $^{11}B(I = {}^3/_2)$ atoms. Note the phase consistency between Z_1 and XY_2; XY_1 and Z_2.

recording ESR absorption spectra of the matrix sample. Windows located in the sides of the apparatus directly across from the boron target and matrix deposition surface were gradually coated by the sputtered boron. The ability to observe the gradual growth of these thin films during the initial series of experiments for a new target is helpful in establishing the optimum laser sputtering conditions.

Results

The overall ESR spectrum assigned to $^{11}B_2$ in its $^3\Sigma_g^-$ ground electronic state is shown in Figure 2 for an argon matrix sample at 5 ± 1 K. Except for $BO(X^2\Sigma)$,[17] B atoms,[2] and the commonly occurring back-ground impurities H, CH_3, and HCO, no other ESR signals were detected in the 0–9400-G range. The observed ESR spectrum of $^{11}B_2$ clearly exhibits all the expected characteristics for a randomly oriented, axially symmetric $^3\Sigma$ radical with two equivalent $I = {}^3/_2$ nuclei. The septet pattern resulting from the ^{11}B nuclear hyperfine interaction (hfi) is clearly resolved on the two perpendicular transitions ($\theta = 90°$; labeled XY_1 and XY_2 in Figure 2) and the low-field $\Delta M_s = 2$ transition which is usually observed for $^3\Sigma$ radicals with a relatively small zero-field splitting (zfs).

Table I. Magnetic Parameters and Line Positions (Gauss) for $^{11}B_2(X^3\Sigma)$ in Neon and Argon Matrices at 4 K

	argon		neon	
	obsd[a]	calcd	obsd[a]	calcd
Z_1	2134 (3)	2131		
XY_1	2702 (1)[b]	2702	2654 (1)[b]	2655
XY_2	4024 (1)[b]	4024	4055 (1)[b]	4055
Z_2	4722 (3)	4724		
$\Delta M_s = 2$	1541 (1)[b]	1541		

Argon Matrix: $g_\parallel = g_\perp = 2.0015$ (4); $D = 3633$ (3) MHz

^{11}B: $|A_\parallel| = 11$ (1) MHz and $|A_\perp| = 27.4$ (3) MHz

Neon Matrix: $D = 3840$ (3) MHz

^{11}B: $|A_\perp| = 26.6$ (3) MHz

[a] Microwave frequency is 9601.4 (4) MHz. Z_1 and Z_2 refer to the parallel lines ($\theta = 0°$) while XY_1 and XY_2 refer to the perpendicular lines ($\theta = 90°$) of the $\Delta M_s = \pm 1$ transitions, where θ is the angle between the applied magnetic field and the molecular axis of B_2. [b] Resolved into septet nuclear hf pattern for two equivalent $^{11}B(I = {}^3/_2)$ atoms in $^{11}B_2$.

The parallel lines ($\theta = 0°$) labeled Z_1 and Z_2 are considerably broader and weaker as expected for a powder sample and do not show resolved nuclear hyperfine structure. The Z_1 parallel line belongs to the same ΔM_s transition as XY_2 and hence these two components show the expected phase characteristics in the first derivative absorption mode. A similar phase consistency is observed for Z_2 and XY_1. The weaker lines labeled "S" in Figure 2 are assigned to parallel lines of $^{11}B_2$ in an alternate trapping site in the argon lattice having a zfs or D parameter approximately 2% larger. It is well-established that this spin–spin interaction parameter is sensitive to environmental effects.[11] Multiple site features are more readily resolved on the parallel lines since these are separated by $2D$ relative to a separation of approximately D for the perpendicular lines. Going from argon to neon matrices, the D parameter for B_2 was observed to increase by about 6%. The trend toward larger D values for $^3\Sigma$ radicals in the more inert rare gas matrices has been observed in other cases.[11]

The method described by Wasserman, Snyder, and Yager for measuring ESR line positions of powder triplet radicals was employed for these $^{11}B_2$ matrix results.[18] The observed and calculated line positions for neon and argon matrices are compared in Table I, which also lists the magnetic parameters obtained by the following exact diagonalization analysis procedure. Since the ^{11}B nuclear hfi is extremely small relative to the applied fields and to D, the values of $g_\parallel$, $g_\perp$, and D were obtained by fitting the centers of the observed transitions with calculated positions using solutions to the following axially symmetric spin Hamiltonian:

$$\hat{H} = g_\perp\beta(H_xS_x + H_yS_y) + g_\parallel\beta(H_zS_z) + DS_z^2 - {}^2/_3D$$

where D is the zero-field parameter (zfs) and the other symbols have their usual meaning. Exact line position equations for the simple triplet case have also been derived previously.[18] The values of the three magnetic parameters can be unambiguously determined since all five features of the $^3\Sigma$ pattern were observed in the argon matrix. Weaker signals were observed for neon matrices, and only the more intense perpendicular lines could be detected. See Table I.

The $A_\perp$ parameter for ^{11}B in B_2 can be obtained directly from the clearly resolved nuclear hfs on the perpendicular XY lines for both neon and argon matrices and has values of 9.5 (1) and 9.8 (1) G, respectively. Figure 3 shows an expanded scale comparison of the observed and simulated ^{11}B septet nuclear hfs for the $\Delta M_s = -1$ perpendicular line with the expected intensity distribution of 1–2–3–4–3–2–1. The simulated spectrum was obtained by adding the $\vec{I}\cdot\mathbf{A}\cdot\vec{S}$ nuclear hyperfine term to the above spin Hamiltonian and solving the resulting 48 × 48 determinants for the transition energies and probabilities by an exact diagonalization

(17) Knight, L. B., Jr.; Wise, M. B.; Davidson, E. R.; McMurchie, L. E. *J. Chem. Phys.* **1982**, *76*, 126.

(18) Wasserman, E.; Snyder, L. C.; Yager, W. A. *J. Chem. Phys.* **1964**, *41*, 1763.

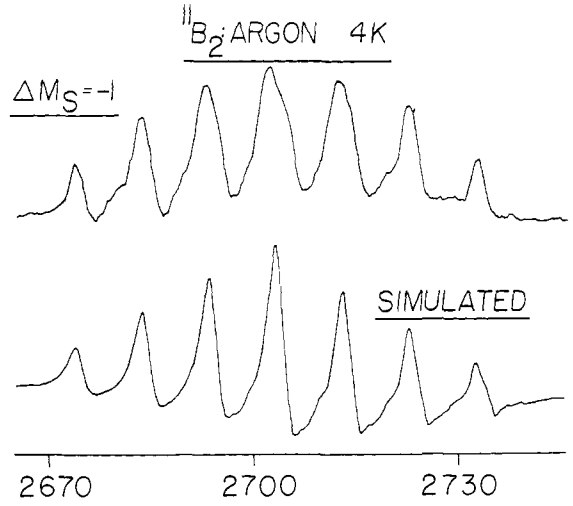

Figure 3. A comparison is presented between a computer simulated spectrum of the $^{11}B(I = {}^3/_2)$ nuclear hyperfine structure in $^{11}B_2$ and an experimental spectrum for the low field perpendicular (θ = 90°) transition—the XY_1 transition shown in the overail $^{11}B_2$ spectrum in Figure 2. The simulated spectrum was generated from an exact diagonalization solution to the spin Hamiltonian. See text.

procedure. The results of this process yield the resonance fields as a function of θ, the angle between the molecular axis and the applied magnetic field. A first derivative Lorentzian line shape program is then used to obtain the simulated spectrum shown in Figure 3.

Since the Z parallel lines for B_2 were too weak and broad to show clearly resolved nuclear hfs, the ^{11}B:$A_\parallel$ parameter was determined in the following manner. It was observed that the septet nuclear hyperfine structure on the $\Delta M_s = 2$ line, centered at 1541 G, had an equal spacing of 8.2 (1) G. Since this transition is a complicated mixture of the various resonance fields between θ = 0° and 90°, it is possible to determine the value of $A_\parallel$ required to reproduce the observed spacing since $A_\perp$ is accurately known from the $\Delta M_s = \pm 1$ lines. With use of the exact simulation procedure described above, the absolute values of $A_\parallel$ were found to be 4.0 ± 0.4 G in argon. Given the anisotropic nature of this $\Delta M_s = 2$ transition, it is rather unusual to observe clearly resolved nuclear hyperfine structure. The virtual lack of **g** tensor anisotropy resulting from a small boron spin–orbit parameter is probably responsible for this fortunate situation, otherwise $A_\parallel$ and A_{dip} for B_2 could not be determined from these spectra. This indirect procedure seems to yield a reasonable $A_\parallel$ value since A_{dip}, which depends on $A_\perp$ and $A_\parallel$, shows excellent agreement with theoretical results.

Multiple trapping sites and lines of the isotopic combination, $^{11}B^{10}B$, probably account for the weaker features observed on the $\Delta M_s = 2$ transition since these lines would be contained within the $^{11}B_2$ signals. (See Figure 2.) The $^{10}B_2$ radical would not be detected since it is present in only 3.5% of abundance (^{10}B; I = 3). The use of very low modulation conditions did show a few weak lines and shoulders on the strong septet lines of $^{11}B_2$ for the $\Delta M_2 = \pm 1$ perpendicular transitions. These probably result from the $^{11}B^{10}B$ radical present in 31% abundance and would have a quartet of septets nuclear hyperfine pattern. However, the larger number of hyperfine lines for this isomer reduces their individual intensities relative to each member of the septet pattern for $^{11}B_2$.

Discussion

It is interesting that high-quality ESR spectral results can be obtained from matrix samples prepared by the pulsed sputtering generation process in conjunction with a continuous flow of matrix gas at conventional rates. ESR results for several neutral and ion radicals prepared by both conventional (continuous generation methods) and pulsed laser generation techniques have recently been compared in our laboratory. No significant ESR spectral differences have been observed except that in some cases the laser method is more convenient and produces significantly greater ESR signal intensities. Specific comparisons of the two generation methods have been conducted for the following cases: AlO,[19] AlHOH,[10] H_2O^+,[20] Cu atoms,[21] HCO,[22] BO,[17] B atoms,[2] CH_3CHO^+,[23] N_2^+,[14] BF^+,[9] and AlF^+.[8] The B atom ESR spectrum observed in these pulsed laser matrix studies was practically identical with that reported by Graham and Weltner, who employed a continuous method—conventional high-temperature vaporization of boron at 2200 K.[2]

Table II. Theoretical Results[a] for the Boron Atom (^2P)

	S&Y[b]	MRSD-CI
SCF energy	−24.5291	−24.5290
Cl energy	−24.6500	−24.6446
K-shell energy	−0.0420	−0.0381
KL-intershell energy	−0.0111	−0.0089
L-shell energy	−0.0720	−0.0709
A_{iso}[c]		−1.78 MHz
A_{aniso}		113.50 MHz

[a] Energies are in hartrees. [b] Sazaki and Yoshimine using an (s,p,d,-f,g,h,i) STO basis SDTQ-Cl. The estimated empirical correlation energy is −0.1247 hartree, ref 28. [c] The experimental hyperfine values in Ar matrix are A_{iso} = 19 MHz, A_{aniso} = 108 MHz, ref 2.

A Tensor: Comparison with Simple Theory. Details of various ab initio calculations for the nuclear hyperfine parameters in $^{11}B_2$ are presented in a later section. The application of the simpler and commonly applied free atom comparison method (FACM) to $^{11}B_2$ is presented first to show that the experimental value of the dipolar interaction is consistent with that expected for the electronic structure which places the two unpaired electrons in p orbitals for the $^3\Sigma_g^-$ ground state ($1\sigma_g^2 1\sigma_\mu^2 2\sigma_g^2 2\sigma_\mu^2 \pi_{xu}^1 \pi_{yu}^1$). The difference in the ^{11}B hfi measured parallel and perpendicular to the molecular symmetry axis is independent of the isotropic (A_{iso}) splitting which is expected to be quite small for a p-type radical.

The axial symmetry of the B_2 radical and the requirement that the trace of the dipolar tensor be zero produces only one independent dipolar parameter: $A_{zz} = -2A_{xx} = -2A_{yy}$. Expressing the observed ESR hyperfine parameters in this manner for a given magnetic nucleus in B_2 yields

$$A_\parallel = A_{iso} + A_{zz} \text{ and } A_\perp = A_{iso} + A_{xx} = A_{iso} - A_{zz}/2$$

where $A_{zz} = \int P_s(3z^2 - r^2)/r^5 \, d\gamma$ and

$$A_{iso} = {}^8/_3 \pi g_e g_n \beta_e \beta_n \langle \delta(r) \rangle$$

which is evaluated over the total spin density (P_s). The above equations show $A_{zz} = 2(A_\parallel - A_\perp)/3$. The experimentally determined value of $2(A_\parallel - A_\perp)/3$ will now be compared with A_{zz} calculated at the SCF level where A_{iso} is zero for the formal assignment of the unpaired electrons to $2p_x$ and $2p_y$ orbitals.

The argon matrix results for $^{11}B_2$ presented in the previous section show that $A_\parallel = \pm 4.0$ (4) G and $A_\perp = \pm 9.8$ (1) G. These ESR results alone cannot determine the absolute signs, but the most reasonable choice (for $A_{iso} < 0$) is $A_\parallel < 0$ and $A_\perp > 0$ on the basis of the following dipolar characteristics of a p-type orbital. The dipolar hyperfine interaction along the bond axis (A_{zz}) is clearly negative since this direction is perpendicular to the symmetry axes of both the $2p_x$ and $2p_y$ boron orbitals. For axial symmetry, all directions perpendicular to the bond axis have the same dipolar interaction. For simplicity, consider the perpendicular direction along the symmetry axis of the $2p_x$ orbital. In this particular perpendicular direction, the dipolar contribution from a $2p_x$ electron is positive and twice the magnitude of the negative contribution from the $2p_y$ electron. Hence, $A_\perp$ would be positive provided A_{iso} is relatively small. These absolute sign assignments yield $2(A_\parallel - A_\perp)/3 = -26$ (1) MHz or $A_{zz} = -26$ (1) MHz, which shows excellent agreement with the various ab

(19) Knight, L. B., Jr.; Weltner, W., Jr. *J. Chem. Phys.* **1971**, *55*, 5066.
(20) Knight, L. B., Jr.; Steadman, J. *J. Chem. Phys.* **1983**, *78*, 5940.
(21) Kasai, P. H.; McLeod, D., Jr. *J. Chem. Phys.* **1971**, *55*, 1566.
(22) Adrain, F. J.; Cochran, E. L.; Bowers, V. A. *J. Chem. Phys.* **1962**, *36*, 1661.
(23) Knight, L. B., Jr.; Williams, F., to be published.

Table III. Total Energies and Hyperfine Properties for B_2 ($^3\Sigma_g^-$)[a]

wave function	config	energy	A_{iso}	A_{aniso}
SCF	1	-49.0903	0.0	-19.48
singles CI	315	-49.1015	-12.72	-22.72
K-orbital MR SD-CI	30675	-49.3673	-3.18	-24.43
INO MR SD-CI	35341	-49.3673	-2.74	-24.42
exptl			15	-26

[a] Calculations were performed at the experimental geometry, R = 1.590 Å. The energy is given in hartrees and the hyperfine properties are in terms of MHz for ^{11}B.

initio results presented in Table III.

A value for A_{zz} in $^{11}B_2$ can also be computed from various boron atomic values of $\langle r^{-3}\rangle_{2p}$ which are commonly used to interpret ESR hyperfine results. Normalizing the total spin density to unity, distributing it equally over both nuclei in both the p_x and p_y orbitals, and including the proper angular factors for a p-orbital yields $A_{zz} = -^1/_5\langle r^{-3}\rangle$. Morton and Preston's[24] values of $\langle r^{-3}\rangle$ yield A_{zz} = -31.8 MHz; a more recent compilation of $\langle r^{-3}\rangle$ values by Koh and Miller[25] yields A_{zz} = -26.7 MHz. In these approximate calculations of A_{zz} which show excellent agreement with the experimental results of -26 (1) MHz, the contribution of two-center integrals was ignored. This is reasonable since the B_2 bond length is large and the dipolar operator varies as r^{-3}.

Theoretical Calculations. SCF and CI calculations were performed on B_2 at the experimental $^3\Sigma_g^-$ geometry (R = 1.590 Å) given by Huber and Herzberg.[26] A Gaussian basis set suitable for calculating hyperfine properties was derived from the energy-optimized, even-tempered (14s,7p) set.[27] Experience has shown that if Gaussian exponents are chosen solely on the basis of energy minimization criteria the "small r" region of space is weighted too heavily. Thus, a supplemental set of diffuse s and p functions was added to produce a (15s,8p) primitive basis. In an even-tempered sequence the ith exponent, ζ_i, is given in terms of two parameters, α and β, as $\zeta_i = \alpha\beta^i$, where i = 1 to N. The particular parameters which were used are α_s = 0.029 291, β_s = 2.580 41, α_p = 0.021 929, β_p = 2.801 07. Exponents for the diffuse functions were obtained by simply extending the even-tempered sequence to begin at $\alpha\beta^0$. This basis is sufficiently large to reproduce the Hartree-Fock limit energy of boron to within 0.0001 hartree (1 hartree = 627.5 kcal/mol).

In order to decrease the computational expense the seven tightest s primitives were contracted by using coefficients taken from the boron 1s atomic orbital, while the p space was left uncontracted. The relatively small degree of contraction was necessitated by the requirement for balancing the inner shell and valence correlation contributions to the isotropic hyperfine property, A_{iso}. Since these effects are of opposite sign and are roughly equal in magnitude a failure to maintain core/valence balance would result in a poor theoretical value of the property. The need to correlate both core and valance regions of space to approximately the same extent translated into a need for both tight s functions (radial correlation) and p functions (angular correlation). The $\langle r\rangle$ of the boron 1s is 0.33 au while the tightest s funtion (the seven-term contraction) and the tightest p function have $\langle r\rangle$ = 0.1 and 0.2, respectively.

The basis set was further enlarged with several groups of higher angular momentum functions (d- and f-type) which perform the dual role of allowing deformation of the atomic densities in the molecular environment and providing angular correlation even for the free atom. The exponents chosen are ζ_d = 2.78, 0.90, and 0.29 and ζ_f = 0.71. The s component of the six cartesian d functions was transformed out, so that the final set, which could be denoted as (15s,8p,3d,1f) → [9s,8p,3d,1f], contained 116 functions for B_2.

Calculations were performed on the ^2P state of the boron atom in an attempt to calibrate the molecular basis set and CI methodology prior to beginning work on B_2. Results from these preliminary calculations are given in Table II along with the large Slater basis set SDTQ-CI calculations of Sazaki and Yoshimine.[28] The latter calculations were done in full atomic symmetry, while our calculations utilized the D_{2h} point group. Because it was intended for use in a molecule the Gaussian basis set used in the boron atom calculations was much smaller than Sazaki and Yoshimine's (8s,7p,6d,5f,4g,3h,2i) STO basis. Nonetheless, the total CI energy produced by the Gaussian basis (-24.645) comes within 5 mhartrees of the STO result. This corresponds to 96% of the estimated empirical correlation energy.

Breaking down the correlation energy into K-shell, KL-intershell and L-shell components shows that the Gaussian basis recovers about 4 mhartrees less inner shell (K-shell) correlation energy than the STO basis and about 1 mhartree less valence correlation (L-shell). The relative weakness of the basis in the core region is primarily due to a lack of tight d and f functions.

Some sensitivity was observed in the boron atom isotropic hyperfine coupling constant to the type of CI wave function. Hartree-Fock singles and doubles CI (HF SD-CI) gave A_{iso} = -9.4 MHz. Multireference SD-CI (MR SD-CI) employing 26 reference configurations reduced the value to -1.8 MHz, compared to an experimental value[2] of A_{iso} = 19 MHz obtained in an Ar matrix at 4 K. The anisotropic components were in much better agreement (calculated 113 MHz, experimental 108 MHz).

It is difficult to know what to make of the discrepancy between the theoretical and experimental values of A_{iso}. On the one hand we know that the current basis set misses 10% of the core correlation energy. A valence-only CI produces a value of +86 MHz for A_{iso}. Thus, the small final value obtained from the core + valence CI is the result of almost perfect cancellation of opposing effects which are nearly two orders of magnitude larger. Since the contribution of the core electrons to A_{iso} is negative it might be naively assumed that recovery of a larger percent of the core correlation would only serve to make the computed value more negative. Absolute agreement between theory and experiment was not much better for the methyl radical, CH_3, where the odd electron occupies a p orbital much like in the boron atom.[29] The ab initio CI number was approximately 13 MHz smaller than the experimental value of 76 MHz.

On the other hand, experimental determinations of A_{iso} for ^2P states are quite difficult due to the perturbing effects of the matrix. For example, measurements of A_{iso} for ^{27}Al (^2P) in four different rare gas matrices produced values ranging from -24 MHz to ~0 MHz.[11]

Some of the same difficulties experienced in the atom are present in the molecule. The B_2 SCF configuration, $1\sigma_g^2 1\sigma_u^2 2\sigma_g^2 2\sigma_u^2 1\pi_{xu}^1 1\pi_{yu}^1$ ($^3\Sigma_g^-$) has both unpaired electrons in orbitals with nodes through the boron nuclei, so there can be no direct contribution to A_{iso}. This is reflected in the 0.0 entry for A_{iso} in Table III. A_{aniso} is in qualitative agreement with experiment. The current SCF energy of -49.0903 hartrees is within a fraction of a millihartree of two previously published (s,p,d,f) Slater-type orbital calculations[5,30] at the same geometry, the lowest being -49.0909 hartrees.

Single-excitation CI is a widely used method for introducing so-called spin polarization effects into the wave function. It is precisely because RHF does not allow the unpaired spins to "polarize" or build up excesses of spin up in one part of the molecule and spin down in other parts that RHF produces a zero value of A_{iso}. The properties obtained from a singles CI calculation are shown in Table III. A_{aniso} is increased slightly compared to the SCF, while A_{iso} is almost equal in magnitude to the experi-

(24) Morton, J. R.; Preston, K. F. *J. Magn. Reson.* **1978**, *30*, 577.
(25) Koh, A. K.; Miller, D. J. *At. Data Nucl. Data Tables* **1985**, *33*, 235.
(26) Huber, K. P.; Herzberg, G. In *Molecular Spectra and Molecular Structure. IV. Constants of Diatomic Molecules*; Van Nostrand-Reinhold Co.: New York, 1979.
(27) Schmidt, M. W.; Ruedenberg, K. *J. Chem. Phys.* **1979**, *71*, 3951.
(28) Sazaki, F.; Yoshimine, M. *Phys. Rev. A.* **1974**, *9*, 17.
(29) Feller, D.; Davidson, E. R. *J. Chem. Phys.* **1984**, *80*, 1006.
(30) *Natl. Bur. Stand, (U.S.) Tech. Note* **1966**, 438.

Table IV. Orbital Occupancy of the Reference Configurations

K-orbital CI Reference Space

	σ_g					π_{ux}	π_{uy}	σ_u					π_{gx}	π_{gy}
	1	2	3	4	5	1	1	1	2	3	4	5	1	1
1	2	2				1	1	2	2					
2	2	2	2			1	1	2						
3	2	2	1				1	2	1				1	
4	2	2	1			1		2	1					1
5	2	2						2	2				1	1
6	2	1				2	1	2	1				1	
7	2	1				1	2	2	1					1
8	2	2				1	1	2					2	
9	2	2				1	1	2						2

Iterative Natural Orbital CI Reference Space

	σ_g					π_{ux}	π_{uy}	σ_u					π_{gx}	π_{gy}
	1	2	3	4	5	1	1	1	2	3	4	5	1	1
1	2	2				1	1	2	2					
2	2	2	2			1	1	2						
3	2	2	1				1	2	1				1	
4	2	2	1			1		2	1					1
5	2	2	1	1		1	1	2						
6	2	2		1	1	1	1	2						
7	2	2				1	1	2	1			1		
8	2	2						2	2				1	1
9	2	1				2	1	2	1				1	
10	2	1				1	2	2	1					1
11	2	1	1			1	1	2	2					
12	2	2				1	1	2						2
13	2	2				1	1	2					2	

mental value but of opposite sign. Singles CI, like unrestricted Hartree–Fock (UHF), is known[29] to overestimate spin polarization effects and, thus, lead to values of A_{iso} which are too large.

More extensive recovery of correlation effects was achieved by means of MR SD–CIs with canonical HF occupied/K-orbital virtual MOs.[31] Transformation of the virtual space to K-orbitals has been shown to produce a set of MOs that mimic the frozen natural orbitals. Configurations were selected for inclusion in the reference space based on the size of their CI expansion coefficient in preliminary runs. Due to the large number of configurations (1–2 million), second-order perturbation theory was used to select the energetically most important double excitations for inclusion in the variational CI. On the basis of perturbation theory predictions, over 95% of the correlation energy present in the 1–2 million configuration was recovered with configuration lists of order 30000–40000. All single excitations, which are important for obtaining good spin and charge density property values, were automatically included.

The K-orbital MR SD–CI computed energy and spin properties are shown in Table III. While the anisotropic hyperfine value is in relatively good agreement with experiment, the isotropic value is considerably smaller than experiment and opposite in sign, as was the case for the boron atom. In fact both the theoretical and experimental values of A_{iso} have changed very little from B to B_2.

Because the $^3\Sigma_g^-$ potential curve is relatively flat (experimental w_e = 1035 cm^{-1}), the effects of vibrational averaging were investigated as a possible source of error. With use of a 3-point Gauss–Hermite numerical interpolation scheme the vibrational averaging correction to a_{iso} was found to be less than 1% and, thus, completely negligible.

As a test of the adequacy of the K-orbitals MOs for simultaneously correlating the core and valence regions, we constructed a set of iterative natural orbitals (INOs)[32] in two stages. First, a core-correlating set containing two σ_g, two σ_u, a $\pi_u(x,y)$, and a $\pi_g(x,y)$ was derived from a singles and doubles CI out of the $1\sigma_g$ and $1\sigma_u$ orbitals. Next a valence set was iteratively generated by HF SD–CIs and finally MR SD–CIs. All Hartree–Fock occupied orbitals were frozen in this procedure.

The inclusion of a multireference CI in the INO process should allow for some orbital relaxation in the presence of the important double excitation ($2\sigma_u^2 \rightarrow 3\sigma_g^2$). This is the second configuration listed in Table IV and appears in the final INO MR SD–CI with an expansion coefficient of 0.27. Two other doubles (simultaneous singles in the σ and π space) which were included in the INO generating process also appeared with final CI expansion coefficients larger than 0.12.

The results in Table III show essentially the same hyperfine properties as the earlier MR SD–CI. Moreover, this particular INO set was slightly less effective energetically than the original canonical/K-orbital set, since it required almost 5000 more spin-adapted configurations to obtain the same energy. It may be that the INOs resulted in perturbation theory being slightly less accurate in selecting the small contributions. Table V contains selected other one-electron properties obtained with the INO CI.

Table V. Selected One-Electron Properties for B_2 in Atomic Units

property	value
$\langle r^2\rangle_e = \langle\sum r_i^2\rangle^a$	51.388
$\langle\delta(B)\rangle_e = \langle\sum\delta(r_{iB})\rangle^a$	69.928
$\langle 1/r_B\rangle_e = \langle\sum(1/r_{iB})\rangle^a$	13.058
$\langle qz/r^3\rangle = \langle\sum q_i z_{iB}/r_{iB}^3\rangle^{b,c}$	0.0017
$B_{zz} = \langle\sum q_i(3z_i^2 - r_i^2)/2\rangle^b$	0.7764
$q_B = \langle\sum q_i(3z^2 - r_i^2)/r_{iB}^5\rangle^b$	−0.0035

[a] The sum runs over all electrons. [b] The sum runs over all electrons and all nuclei. [c] The Hellman–Feyman force on the nuclei will be zero at the equilibrium geometry for a full CI with a complete basis set.

Acknowledgment. Project support (L.B.K.) from the National Science Foundation (CHE-8508085) and student support from the Camille and Henry Dreyfus Foundation and the General Electric Foundation are gratefully acknowledged. Theoretical aspects (E.R.D.) of this work were also supported in part by a National Science Foundation grant. An equipment grant from the Pew Memorial Trust to Furman University is gratefully acknowledged.

Registry No. $^{11}B_2$, 106694-41-1.

(31) Feller, D.; Davidson, E. R. *J. Chem. Phys.* **1981**, *84*, 3977.

(32) Bender, C. F.; Davidson, E. R. *J. Phys. Chem.* **1966**, *70*, 2675.